



# **O<sub>2</sub> : CO<sub>2</sub> exchange ratio for net turbulent flux observed in an urban area of Tokyo, Japan, and its application to an evaluation of anthropogenic CO<sub>2</sub> emissions**

Shigeyuki Ishidoya<sup>1</sup>, Hirofumi Sugawara<sup>2</sup>, Yukio Terao<sup>3</sup>, Naoki Kaneyasu<sup>1</sup>, Nobuyuki Aoki<sup>1</sup>, Kazuhiro Tsuboi<sup>4</sup>, and Hiroaki Kondo<sup>1</sup>

<sup>1</sup>National Institute of Advanced Industrial Science and Technology (AIST), Tsukuba 305-8569, Japan

<sup>2</sup>Department of Earth and Ocean Sciences, National Defense Academy of Japan, Yokosuka 239-8686, Japan

<sup>3</sup>National Institute for Environmental Studies, Tsukuba 305-8506, Japan

<sup>4</sup>Meteorological Research Institute, Tsukuba 305-0052, Japan

**Correspondence:** Shigeyuki Ishidoya (s-ishidoya@aist.go.jp)

Received: 17 July 2019 – Discussion started: 5 September 2019

Revised: 23 April 2020 – Accepted: 24 April 2020 – Published: 15 May 2020

**Abstract.** In order to examine O<sub>2</sub> consumption and CO<sub>2</sub> emission in a megacity, continuous observations of atmospheric O<sub>2</sub> and CO<sub>2</sub> concentrations, along with CO<sub>2</sub> flux, have been carried out simultaneously since March 2016 at the Yoyogi (YYG) site located in the middle of Tokyo, Japan. An average O<sub>2</sub> : CO<sub>2</sub> exchange ratio for net turbulent O<sub>2</sub> and CO<sub>2</sub> fluxes (OR<sub>F</sub>) between the urban area and the overlying atmosphere was obtained based on an aerodynamic method using the observed O<sub>2</sub> and CO<sub>2</sub> concentrations. The yearly mean OR<sub>F</sub> was found to be 1.62, falling within the range of the average OR values of liquid and gas fuels, and the annual average daily mean O<sub>2</sub> flux at YYG was estimated to be  $-16.3 \mu\text{mol m}^{-2} \text{s}^{-1}$  based on the OR<sub>F</sub> and CO<sub>2</sub> flux. By using the observed OR<sub>F</sub> and CO<sub>2</sub> flux, along with the inventory-based CO<sub>2</sub> emission from human respiration, we estimated the average diurnal cycles of CO<sub>2</sub> fluxes from gas and liquid fuel consumption separately for each season. Both the estimated and inventory-based CO<sub>2</sub> fluxes from gas fuel consumption showed average diurnal cycles with two peaks, one in the morning and another one in the evening; however, the evening peak of the inventory-based gas consumption was much larger than that estimated from the CO<sub>2</sub> flux. This can explain the discrepancy between the observed and inventory-based total CO<sub>2</sub> fluxes at YYG. Therefore, simultaneous observations of OR<sub>F</sub> and CO<sub>2</sub> flux are useful in validating CO<sub>2</sub> emission inventories from statistical data.

## **1 Introduction**

Precise observation of the atmospheric O<sub>2</sub> concentration (O<sub>2</sub>/N<sub>2</sub> ratio) has been carried out since the early 1990s to elucidate the global CO<sub>2</sub> cycle (Keeling and Shertz, 1992). The approach is based on the  $-\text{O}_2 : \text{CO}_2$  exchange ratios (oxidative ratio;  $\text{OR} = -\Delta\text{O}_2/\Delta\text{CO}_2$  mol mol<sup>-1</sup>) for the terrestrial biospheric activities and fossil fuel combustion. The OR value of 1.1 has been used widely for the terrestrial biospheric O<sub>2</sub> and CO<sub>2</sub> fluxes (Severinghaus, 1995). On the other hand, the ORs of 1.95 for gaseous fuels, 1.44 for oil and other liquid fuels, and 1.17 for coal or solid fuels are usually used (Keeling, 1988). Therefore, OR is a useful indicator of cause(s) of the observed variations in the atmospheric O<sub>2</sub> and CO<sub>2</sub> concentrations. The atmospheric CO<sub>2</sub> concentration has been observed not only at remote sites such as Mauna Loa (19.5° N, 155.6° W), Hawaii, USA, to capture a baseline variation in the background air (e.g., Keeling et al., 2011), but also recently in urban areas to estimate CO<sub>2</sub> emissions locally from fossil fuel combustion (e.g., Mitchell et al., 2018; Sargent et al., 2018). For the latter purpose, simultaneous observations of the atmospheric O<sub>2</sub> and CO<sub>2</sub> concentrations should provide important insight into validating the inventory-based CO<sub>2</sub> emissions from gaseous, liquid and solid fuels. Steinbach et al. (2011) estimated a global dataset of spatial and temporal variations of OR for the fossil fuel combustion using the EDGAR (Emission Database for Global Atmospheric Research) inventory and fossil fuel con-

sumption data from the UN energy statistics. The statistically estimated OR should be validated by observed OR; however, observations of the atmospheric O<sub>2</sub> concentration in urban areas are still limited (e.g., van der Laan et al., 2014; Goto et al., 2013a). Moreover, simultaneous observations of the OR and CO<sub>2</sub> flux between an urban area and the overlying atmosphere have never been reported before. Observations of the CO<sub>2</sub> flux have been carried out at various urban stations, such as London, UK (Ward et al., 2013), Mexico City, Mexico (Velasco et al., 2009), Beijing, China (Song and Wang, 2012), and Tokyo, Japan (Hirano et al., 2015), allowing us to observe urban CO<sub>2</sub> emission directly in the flux footprint. Therefore, if the OR for the net turbulent O<sub>2</sub> and CO<sub>2</sub> fluxes (hereafter referred to as “OR<sub>F</sub>”) can be observed, then such information can be used as a useful constraint for evaluating the contributions of the gaseous, liquid, and solid fuels and the terrestrial biospheric activities to the observed CO<sub>2</sub> flux. From the measurements, it also becomes possible to observe the urban O<sub>2</sub> flux by multiplying the CO<sub>2</sub> flux by OR<sub>F</sub>.

In this paper, we first present the simultaneous observational results of the O<sub>2</sub> and CO<sub>2</sub> concentrations and the CO<sub>2</sub> flux in the urban area of Tokyo, Japan. From a relationship between the vertical gradients of the observed O<sub>2</sub> and CO<sub>2</sub> concentrations, we derive OR<sub>F</sub> based on an aerodynamic method (Yamamoto et al., 1999). The present paper follows Ishidoya et al. (2015), who reported OR<sub>F</sub> for the O<sub>2</sub> and CO<sub>2</sub> fluxes between a forest canopy and the overlying atmosphere. We also compare the observed OR<sub>F</sub> with the OR value of the overlying atmosphere above the urban canopy (hereafter referred to as “OR<sub>atm</sub>”) to highlight the characteristics of the O<sub>2</sub> and CO<sub>2</sub> exchange processes in the urban canopy air at the YYG site. Finally, we estimate the average diurnal cycles of CO<sub>2</sub> fluxes from gas and liquid fuel consumption separately by using the OR<sub>F</sub>, CO<sub>2</sub> flux, and inventory-based CO<sub>2</sub> emission from human respiration in order to validate the inventory-based CO<sub>2</sub> emissions from gas consumption and traffic.

## 2 Experimental procedures

### 2.1 Site description

In order to observe the atmospheric O<sub>2</sub> and CO<sub>2</sub> concentrations and CO<sub>2</sub> flux between the urban area and the overlying atmosphere, the instruments were installed on a roof-top tower of Tokai University (52 m above ground, 25 m above roof) at Yoyogi (YYG; 35.66° N, 139.68° E), Tokyo, Japan. The YYG site is a mid-rise residential area and located in the northern part of Shibuya ward, Tokyo. Figure 1 shows the location of the YYG site and the flux footprints averaged for summer and winter runs, calculated by the model of Neftel et al. (2008). The main land cover around the site is characterized by low- to mid-rise residential buildings with a mean height of 9 m. The population density in this area is 16 600

persons per square kilometer. At the YYG site, the prevailing wind is from SW in the summer and NW in the winter. The flux footprint includes a vegetated area of 9 % in the summer and 2 % in the winter, reflecting seasonal changes in the wind direction.

### 2.2 Continuous measurements of the atmospheric O<sub>2</sub> and CO<sub>2</sub> concentrations and CO<sub>2</sub> flux

Observations of the atmospheric O<sub>2</sub> and CO<sub>2</sub> concentrations have been carried out at the YYG site using a continuous measurement system employing a paramagnetic O<sub>2</sub> analyzer (POM-6E, Japan Air Liquid) and a non-dispersive infrared CO<sub>2</sub> analyzer (NDIR; Li-820, LI-COR) since March 2016. The O<sub>2</sub> concentration is reported as the O<sub>2</sub>/N<sub>2</sub> ratio in per meg:

$$\delta(\text{O}_2/\text{N}_2) = \left[ \frac{(\text{O}_2/\text{N}_2)_{\text{sample}}}{(\text{O}_2/\text{N}_2)_{\text{standard}}} - 1 \right] \times 10^6, \quad (1)$$

where the subscripts “sample” and “standard” indicate the sample air and the standard gas, respectively. Because O<sub>2</sub> is about 20.94 % of air by volume (Tohjima et al., 2005a), the addition of 1 μmol of O<sub>2</sub> to 1 mol of dry air increases δ(O<sub>2</sub>/N<sub>2</sub>) by 4.8 per meg (= 1/0.2094). If CO<sub>2</sub> were to be converted one-for-one into O<sub>2</sub>, this would cause an increase of 4.8 per meg of δ(O<sub>2</sub>/N<sub>2</sub>), equivalent to an increase of 1 μmol mol<sup>-1</sup> in O<sub>2</sub> for each 1 μmol mol<sup>-1</sup> decrease in CO<sub>2</sub>. Therefore, the ratio of 4.8 per meg μmol mol<sup>-1</sup> was used to convert the observed δ(O<sub>2</sub>/N<sub>2</sub>) to O<sub>2</sub> concentration relative to an arbitrary reference point. In this study, δ(O<sub>2</sub>/N<sub>2</sub>) values of each air sample were measured with the paramagnetic analyzer using working standard air that was measured against our primary standard air (cylinder no. CRC00045; AIST scale) using a mass spectrometer (Thermo Scientific Delta-V) (Ishidoya and Murayama, 2014).

Sample air was taken at the tower heights of 52 and 37 m using a diaphragm pump at a flow rate higher than 10 L min<sup>-1</sup> to prevent thermally diffusive fractionation of air molecules at the air intake (Blaine et al., 2006). Then, a large portion of the air is exhausted from the buffer, with the remaining air allowed to flow into the analyzers from the center of the buffer. It is then sent to an electric cooling unit with a water trap cooled to -80 °C at a flow rate of 100 mL min<sup>-1</sup>, with the pressure stabilized to 0.1 Pa and measured for 10 min at each height (one-cycle measurements). The method to sample a small subset of air from a high flow rate is similar to those used in Goto et al. (2013b), and we have confirmed that the atmospheric δ(O<sub>2</sub>/N<sub>2</sub>) values observed by the measurement system agree well with those obtained from independent continuous measurements of δ(O<sub>2</sub>/N<sub>2</sub>) using the mass spectrometer (see Fig. 4 in Ishidoya et al., 2017). After nine cycles of measurements (five and four cycles for 37 and 52 m, respectively), high-span standard gas, prepared by adding appropriate amounts of pure O<sub>2</sub> or N<sub>2</sub> to industrially prepared CO<sub>2</sub> standard air,

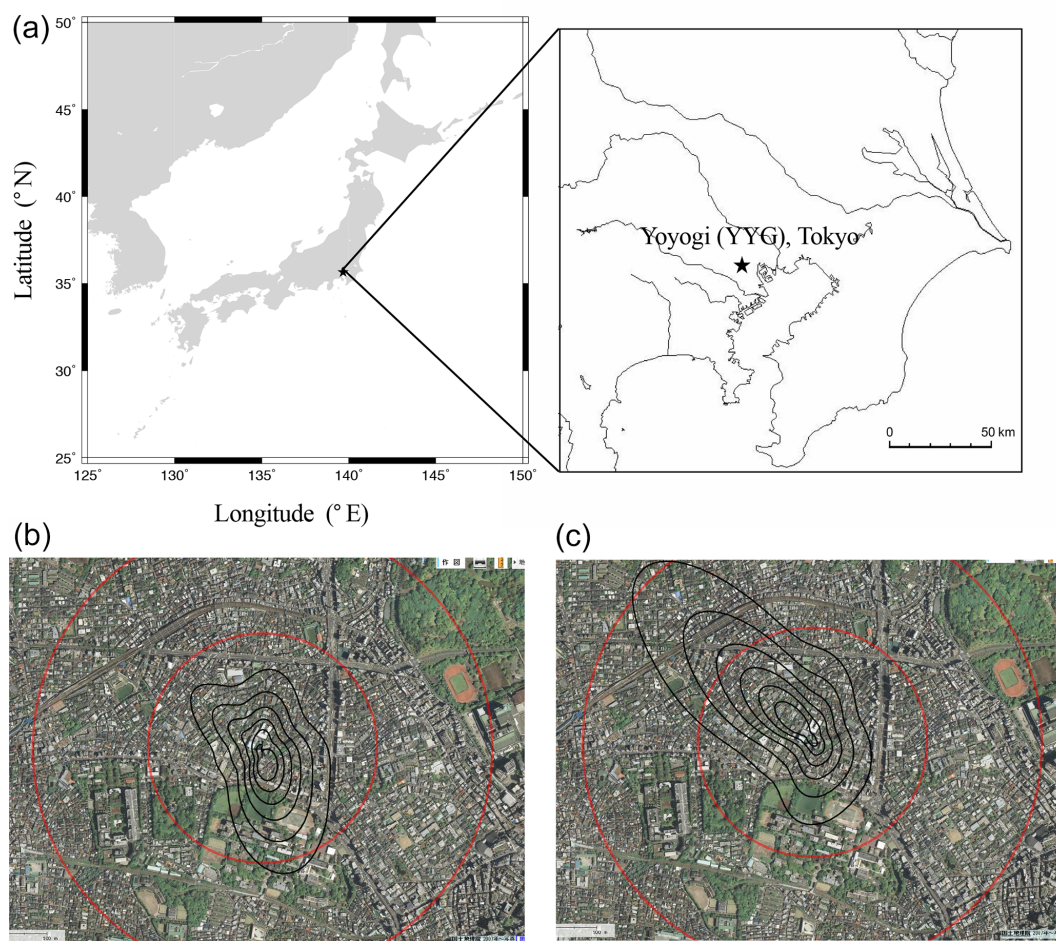


**Figure 1.** (a) Location of the Yoyogi site (35.66° N, 139.68° E, YYG), Tokyo, Japan. (b, c) Aerial photo from the Geospatial Information Authority of Japan around the study area at YYG. Ensemble-mean flux footprints in the summer (b) and winter (c) are also shown by black circles. The contour lines indicate contribution in measured flux (60 %, 50 %, 40 %, 30 %, 20 % and 10 % from outside to inside). Inside and outside the red circles indicate the distances of 500 and 1000 m, respectively, from a roof-top tower of Tokai University where the observations of O<sub>2</sub> and CO<sub>2</sub> concentrations and CO<sub>2</sub> flux were carried out.

was introduced into the analyzers with the same flow rate and pressure as the sample air and measured for 5 min, and then low-span standard gas was measured by the same procedure. The dilution effects on the O<sub>2</sub> mole fraction measured by the paramagnetic analyzer were corrected experimentally, not only for the changes in CO<sub>2</sub> of the sample air or standard gas measured by the NDIR, but also for the changes in Ar of the standard gas measured by the mass spectrometer as  $\delta(\text{Ar}/\text{N}_2)$ . The analytical reproducibility of the  $\delta(\text{O}_2/\text{N}_2)$  and CO<sub>2</sub> concentration achieved by the system was about 5 per meg and 0.06  $\mu\text{mol mol}^{-1}$ , respectively, for 2 min average values. Details of the continuous measurement system used are given in Ishidoya et al. (2017).

It should be noted that we used the gravimetrically prepared air-based CO<sub>2</sub> standard gas system with uncertainties of  $\pm 0.13 \mu\text{mol mol}^{-1}$  on the TU-10 scale (Nakazawa et

al., 1991) to determine CO<sub>2</sub> concentration in this study. The highest concentration of the gravimetrically prepared standard gas was about 450  $\mu\text{mol mol}^{-1}$ , while CO<sub>2</sub> concentrations of more than 600  $\mu\text{mol mol}^{-1}$  were observed in this study. Therefore, we compared the NDIR-based CO<sub>2</sub> concentrations observed in this study with those observed by using cavity ring-down spectroscopy (CRDS; G2401, Picarro) on the NIES-09 scale (Machida et al., 2011) at the YYG site (our unpublished data). Although the highest CO<sub>2</sub> concentration of the gravimetrically prepared standard of the NIES-09 scale is similar to that of the TU-10 scale, a slope of 0.974 ppm ppm<sup>-1</sup> is derived from a least-squares regression line fitted to the relationship between the CO<sub>2</sub> concentrations observed by NDIR on the TU-10 scale and those by CRDS on the NIES-09 scale with a correlation coefficient ( $r$ ) of 0.978. On the other hand, we obtained a slope of 1.002 per meg per

meg<sup>-1</sup> ( $r = 0.999$ ) from the regression line fitted to the relationship between the O<sub>2</sub> concentrations of gravimetrically prepared standard gases (Aoki et al., 2019) measured by the mass spectrometer on the AIST scale and the gravimetric values of the standard gases covering a much wider range than the atmospheric variations in the O<sub>2</sub> concentration. Therefore, the uncertainty in OR due to the span uncertainties of O<sub>2</sub> and CO<sub>2</sub> concentrations is expected to be within 3 %.

In order to observe the CO<sub>2</sub> flux at the YYG site, the turbulence and the turbulent fluctuation of CO<sub>2</sub> were observed at 52 m with a high time resolution of 10 Hz by using a sonic anemometer (WindMasterPro, Gill) and an open-path infrared gas analyzer (LI-7500, LI-COR) starting November 2012. The sensors were located at more than 5 times the mean building height (9 m), and then it was above the urban roughness sublayer. Turbulent flux of CO<sub>2</sub> was calculated by the eddy correlation method using EddyPro<sup>®</sup> (Licor) for every 30 min period. Correlations were applied in the calculation for water-vapor density fluctuation (Webb et al., 1980) and mean vertical wind by using the double rotation algorithm (Wilczak et al., 2001). The calculated flux was filtered for data quality based on the steady test and the integral turbulence characteristics in Aubinet et al. (2012). We used the flag 0–2 data in EddyPro<sup>®</sup> software based on Mauder and Foken (2006).

### 3 Results and discussion

#### 3.1 Variations in the atmospheric O<sub>2</sub> and CO<sub>2</sub> concentrations

We show the 10 min average values of the atmospheric O<sub>2</sub> and CO<sub>2</sub> concentrations observed at the height of 52 m at YYG in Fig. 2. As seen in the figure, O<sub>2</sub> and CO<sub>2</sub> concentrations vary in opposite phase with each other on timescales ranging from several hours to a seasonal cycle. In general, opposite phase variations of atmospheric O<sub>2</sub> and CO<sub>2</sub> are driven by fossil fuel combustion and terrestrial biospheric activities. In contrast, the atmospheric O<sub>2</sub> variation in  $\mu\text{mol mol}^{-1}$  due to the air–sea exchange of O<sub>2</sub> is much larger than that of CO<sub>2</sub> on timescales shorter than 1 year (e.g., Goto et al., 2017; Hoshina et al., 2018); this is because the equilibration time for O<sub>2</sub> between the atmosphere and the surface ocean is much shorter than that for CO<sub>2</sub> due to the influence of the carbonate dissociation effect on the air–sea exchange of CO<sub>2</sub> (Keeling et al., 1993). Therefore, we attribute the opposite phase variations in O<sub>2</sub> and CO<sub>2</sub> observed in this study mainly to fossil fuel combustion and terrestrial biospheric activities. Figure 2 also shows that  $\Delta\text{O}_2$ , obtained by subtracting O<sub>2</sub> at 41 m from that at 52 m on the tower, varies in opposite phase with the corresponding  $\Delta\text{CO}_2$ . High  $\Delta\text{O}_2$  values are more frequently observed in the winter than in the summer, and short-term (several hours to days) decreases in the O<sub>2</sub> concentration are intense in the winter.

To examine a relationship between the appearances of high  $\Delta\text{O}_2$  and O<sub>2</sub> concentration decrease, detail variations in the O<sub>2</sub> and CO<sub>2</sub> concentrations,  $\Delta\text{O}_2$  and  $\Delta\text{CO}_2$  for the periods 16–23 December and 1–9 July 2016, are shown in Fig. 3. As seen in the figure, increases in  $\Delta\text{O}_2$  coincide with decreases in O<sub>2</sub> concentration in December, especially in the nighttime. Such a coincidence is also seen in July; however, the increases in  $\Delta\text{O}_2$  are much smaller than those in December. Therefore, it is highly likely that O<sub>2</sub> is consumed within the urban canopy at YYG, more so in the winter due to an increased usage of gas and/or liquid fuels for heating and to a temperature inversion near the surface. The daily mean CO<sub>2</sub> flux from the urban area to the overlaying atmosphere shown in Fig. 2 shows a seasonal cycle with a wintertime maximum, consistent with the enhancement of O<sub>2</sub> consumption in the urban canopy.

In this study, we focus on the short-term variations of O<sub>2</sub> and CO<sub>2</sub> for periods of several hours to days, to elucidate the O<sub>2</sub> and CO<sub>2</sub> exchange processes between the urban area and the atmosphere by examining two types of OR: one is OR<sub>atm</sub> calculated from a relationship between the O<sub>2</sub> and CO<sub>2</sub> concentration values observed at 52 or 37 m and the other one is OR<sub>F</sub>, for the O<sub>2</sub> and CO<sub>2</sub> fluxes between the urban area and the overlaying atmosphere, calculated from a relationship between  $\Delta\text{O}_2$  and  $\Delta\text{CO}_2$ . The relationships of the O<sub>2</sub> and CO<sub>2</sub> fluxes with OR<sub>F</sub> are based on the aerodynamic method of Yamamoto et al. (1999):

$$F_{\text{O}} = -K \frac{\Delta\text{O}_2}{\Delta z}, \quad (2)$$

$$F_{\text{C}} = -K \frac{\Delta\text{CO}_2}{\Delta z}, \quad (3)$$

$$\text{OR}_F = -\frac{F_{\text{O}}}{F_{\text{C}}} = -\frac{\Delta\text{O}_2}{\Delta\text{CO}_2}. \quad (4)$$

Here,  $F_{\text{O}}$  ( $F_{\text{C}}$ ) ( $\mu\text{mol m}^{-2} \text{s}^{-1}$ ) represents the O<sub>2</sub> (CO<sub>2</sub>) flux from the urban area to the overlaying atmosphere,  $K$  is the vertical diffusion coefficient, and  $\Delta\text{O}_2\Delta z^{-1}$  ( $\Delta\text{CO}_2\Delta z^{-1}$ ) is the vertical concentration gradient of O<sub>2</sub> (CO<sub>2</sub>). The vertical diffusion is a sum of mass-independent eddy and mass-dependent molecular diffusion; however, the effect of molecular diffusion on the observed variations of O<sub>2</sub> and CO<sub>2</sub> concentrations is generally negligible in the troposphere. It is significant in the stratosphere (e.g., Ishidoya et al., 2013a). Therefore, we used the same diffusion coefficient  $K$  for O<sub>2</sub> and CO<sub>2</sub> in Eqs. (2) and (3), which enabled us to estimate  $F_{\text{O}}$  by using the observed  $\Delta\text{O}_2$ ,  $\Delta\text{CO}_2$  and  $F_{\text{C}}$  as in Eq. (4). In general, OR<sub>atm</sub> reflects wider footprints of O<sub>2</sub> and CO<sub>2</sub> than OR<sub>F</sub> due to horizontal atmospheric transport (Schmid, 1994). We note that the definitions of OR<sub>F</sub> and OR<sub>atm</sub> are similar to those of ER<sub>F</sub> and ER<sub>atm</sub>, respectively, reported by Ishidoya et al. (2013b, 2015).



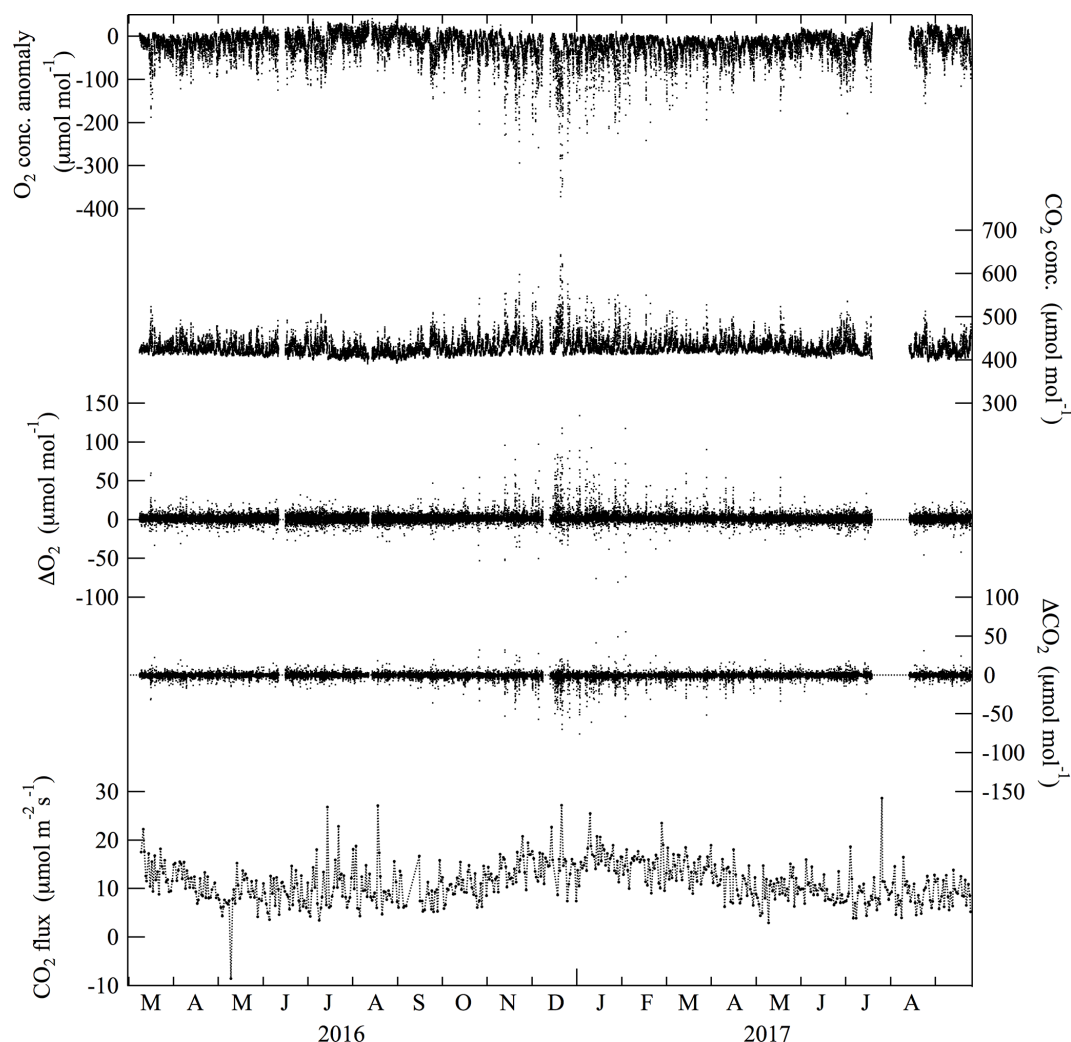


**Figure 2.** Variations in O<sub>2</sub> and CO<sub>2</sub> concentrations observed at the tower height of 52 m at Yoyogi, Tokyo, Japan, for the period March 2016–September 2017. The O<sub>2</sub> concentrations are expressed as deviations from the value observed at 09:58 local time on 9 March 2016.  $\Delta$ O<sub>2</sub>, representing the differences calculated by subtracting the observed O<sub>2</sub> concentrations at 37 m from that at 52 m, are also shown.  $\Delta$ CO<sub>2</sub> are the same as  $\Delta$ O<sub>2</sub> but for CO<sub>2</sub> concentration. Daily mean CO<sub>2</sub> fluxes observed using the eddy correlation method are also shown, and the flux takes on a positive value when the urban area emits CO<sub>2</sub> to the overlaying atmosphere.

In order to calculate OR<sub>atm</sub> for short-term variations, (1) we applied a best-fit curve consisting of the fundamental and its first harmonics (periods of 12 and 6 months) and a linear trend to the maximum (minimum) values of O<sub>2</sub> (CO<sub>2</sub>) observed at 52 m during the successive 1-week periods and regarded the best-fit curve as its baseline variation; (2) then, the baseline variation of O<sub>2</sub> (CO<sub>2</sub>) concentration was subtracted from the respective O<sub>2</sub> (CO<sub>2</sub>) concentrations observed at 52 m. Figure 4 shows the baseline variations and the variations in the O<sub>2</sub> and CO<sub>2</sub> concentrations observed at Minamitorishima (MNM; 24.28° N, 153.98° E), Japan (updated from Ishidoya et al., 2017). MNM is a small and isolated coral island located 1850 km southeast of Tokyo, Japan, and the observation site was operated by the Japan Meteorological Agency (JMA) under the Global Atmosphere

Watch program of the World Meteorological Organization (WMO/GAW). The baseline variations of O<sub>2</sub> and CO<sub>2</sub> at YYG show clear seasonal cycles with peak-to-peak amplitudes of 28 and 16  $\mu\text{mol mol}^{-1}$ , respectively, with a corresponding seasonal maximum and minimum appearing in mid August. The amplitude of the seasonal O<sub>2</sub> (CO<sub>2</sub>) cycle and the appearance of a seasonal maximum (minimum) were found to be larger and earlier, respectively, than those observed at MNM, while the annual average values of the baseline concentration variations of O<sub>2</sub> and CO<sub>2</sub> at YYG did not differ significantly from those at MNM. These characteristics of the seasonal cycles and the annual average values of the baseline variations at YYG and their comparison with those at MNM are generally consistent with those observed at similar latitude over the western Pacific region (Tohshima et

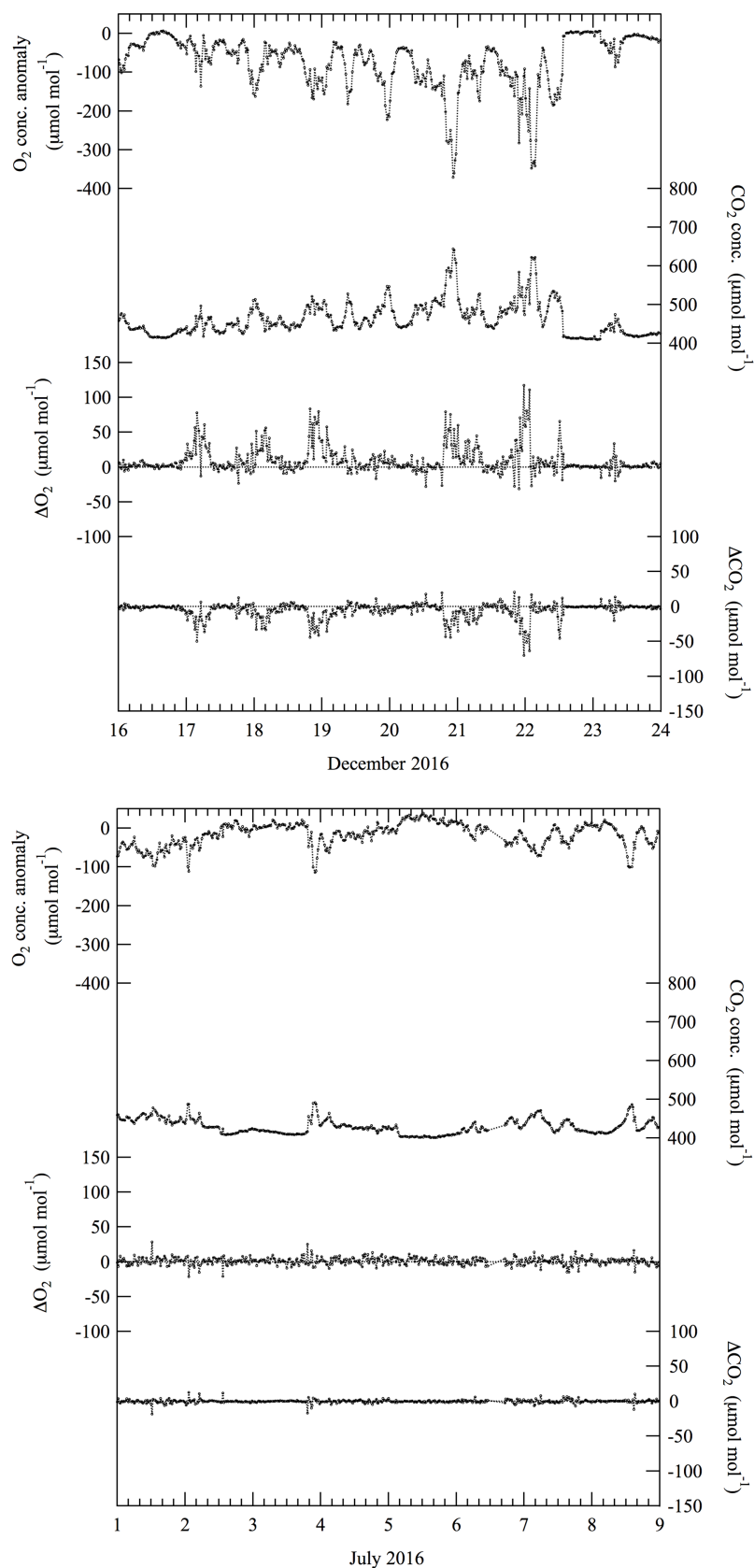


**Figure 3.** Same as in Fig. 2 but for O<sub>2</sub> and CO<sub>2</sub> concentrations, ΔO<sub>2</sub> and ΔCO<sub>2</sub> for the periods 16–23 December and 1–9 July 2016.

al., 2005b). Therefore, in spite of the fact that the YYG site is located in a megacity, the baseline variations of O<sub>2</sub> and CO<sub>2</sub> concentrations are similar to those in the background air.

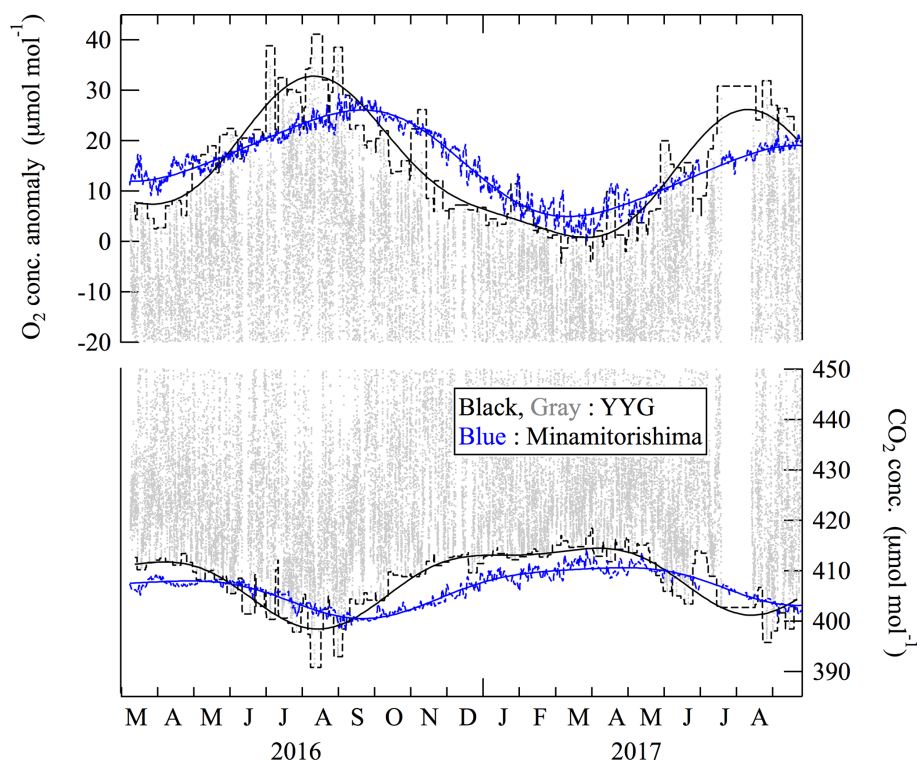
### 3.2 O<sub>2</sub> : CO<sub>2</sub> exchange ratio between the urban area and the overlaying atmosphere

Figure 5a shows the relationship between all the  $\Delta$ O<sub>2</sub> and  $\Delta$ CO<sub>2</sub> values to obtain the average OR<sub>F</sub> throughout the observation period in this study. When errors in both species are non-negligible, a standard least-squares linear regression will give a biased and erroneous slope. Therefore, we apply an unweighted Deming regression analysis to the data (e.g., Linnet, 1993), assuming the ratio between the squared analytical standard deviations to be  $0.06^2/(5 \times 0.2094)^2$  (ppm ppm<sup>-1</sup>) to take into account the measurement uncertainties of CO<sub>2</sub> and O<sub>2</sub> concentrations. We consider the slope obtained by Deming regression to be OR<sub>F</sub>, but we use a standard deviation obtained from a standard least-squares regression to indicate the uncertainty of the slope. The jackknife method (Linnet, 1990) could be used to derive a standard error for Deming regression; however, by using a short dataset extracted from the observed data used in the present study, we confirmed that the standard deviations obtained from an ordinary regression are larger than the errors from the jackknife method. Therefore, using a standard deviation from ordinary regression is reasonable to ensure larger uncertainty for the OR<sub>F</sub>. The average OR<sub>F</sub> value was calculated to be  $1.620 \pm 0.004$  ( $\pm 1\sigma$ ). This value falls within the range of the average OR values of 1.44 for liquid fuels and 1.95 for gas fuels, which suggests that the O<sub>2</sub> and CO<sub>2</sub> fluxes at the YYG site were driven mainly by a consumption of liquid and gas fuels rather than terrestrial biospheric activities of which OR is about 1.1 (Severinghaus, 1995). The relationship between the O<sub>2</sub> and CO<sub>2</sub> concentration anomalies, calculated by subtracting the respective baseline variations shown in Fig. 4 from the observed O<sub>2</sub> and CO<sub>2</sub> concentrations, is also shown in Fig. 5b. By applying the Deming regression analysis to the data, we obtained an average OR<sub>atm</sub> value of  $1.541 \pm 0.002$  ( $\pm 1\sigma$ ) throughout the observation period. The OR<sub>atm</sub> value also falls within the range of the average OR values for liquid fuels and gas fuels. However, the OR<sub>atm</sub> in this figure is not appropriate in representing the OR for the O<sub>2</sub> and CO<sub>2</sub> fluxes around the YYG site since it was determined by using the entire 18 months of collected observations that the site is influenced by various trajectories of air masses with a much wider regional signature than the flux footprints. Therefore, we compare below the OR<sub>F</sub> and OR<sub>atm</sub> values by changing the aggregation periods to calculate the ORs and examine the validity of using OR<sub>F</sub> rather than OR<sub>atm</sub> to evaluate the relationship between the local O<sub>2</sub> and CO<sub>2</sub> fluxes.

Figure 6 shows examples of the OR<sub>F</sub> calculated by applying Deming regression fitted to  $\Delta$ O<sub>2</sub> and  $\Delta$ CO<sub>2</sub> values during the successive 12 h periods observed in January 2017 and July 2016. The corresponding OR<sub>atm</sub> and wind direction

observed for the periods are also shown in the figure. As seen in the figure, variabilities in the OR<sub>F</sub> and OR<sub>atm</sub> are larger in July than in December. The average OR<sub>F</sub>, calculated using the OR values within a range of 0.5 to 2.5, were  $1.65 \pm 0.20$  and  $1.52 \pm 0.32$  in the winter (December to February) and summer (July to September), respectively. The corresponding average OR<sub>atm</sub> values were  $1.61 \pm 0.15$  in the winter and  $1.45 \pm 0.27$  in the summer. To examine the dependency of the OR on the wind direction, we also calculated OR<sub>F</sub> and OR<sub>atm</sub> for the periods when the prevailing wind directions were observed to be from 320 to 360° (NW) and from 180 to 220° (SW) in the winter and summer, respectively. The number of measurements taken during the time of these prevailing winds constituted 30 % (winter) and 8 % (summer) of the total number of measurements. The calculated OR<sub>F</sub>, OR<sub>atm</sub> and prevailing winds are shown by blue dots in Fig. 6. The average OR<sub>F</sub> (OR<sub>atm</sub>) values, calculated using the OR values within a range of 0.5 to 2.5, were  $1.65 \pm 0.25$  ( $1.58 \pm 0.19$ ) in the winter and  $1.58 \pm 0.40$  ( $1.42 \pm 0.33$ ) in the summer, respectively. Therefore, the average OR<sub>F</sub> and OR<sub>atm</sub> calculated using all the values obtained from the 12 h aggregation periods did not differ significantly from those that were calculated using only the data that were associated with the above-mentioned prevailing wind directions. The average OR<sub>F</sub> seems to be slightly higher than OR<sub>atm</sub>; however, their uncertainties are too large to discuss the significance of the slight difference. Taking these facts into consideration, we use all the O<sub>2</sub> and CO<sub>2</sub> concentration data without filtering by the wind direction to increase the number of data points for calculating OR<sub>F</sub> and OR<sub>atm</sub>; this is consistent with the purpose of this study to derive representative OR values at the YYG site in order to validate the CO<sub>2</sub> emission inventory (Hirano et al., 2015). For analyses of specific events, we have reported analytical results of OR<sub>atm</sub> and simultaneously measured PM<sub>2.5</sub> aerosol composition for a week long pollution event at the YYG site (Kaneyasu et al., 2020).

To examine the seasonal difference between the OR<sub>F</sub> and OR<sub>atm</sub> values, we show the OR<sub>F</sub> values calculated by applying regression lines to 1 d and 1-week successive  $\Delta$ O<sub>2</sub> and  $\Delta$ CO<sub>2</sub> values in Fig. 7. The corresponding OR<sub>atm</sub> values, obtained by applying Deming regression fitted to successive O<sub>2</sub> and CO<sub>2</sub> concentration anomalies in Fig. 5b, are also shown. Since there is no statistically significant difference between the two (based on the uncertainties shown in the figure ( $\pm 1\sigma$ )), we focus our discussion on the OR values obtained from the 1-week successive data. Clear seasonal cycles with wintertime maxima are found in both the OR<sub>F</sub> and OR<sub>atm</sub> values at YYG. Larger OR<sub>atm</sub> values in the winter than in the summer in urban areas have been reported by some past studies (e.g., van der Laan et al., 2014; Ishidoya and Murayama, 2014; Goto et al., 2013a) and generally interpreted as a result of the wintertime increase and decrease in fossil fuel combustion and terrestrial biospheric activities, respectively. Biospheric activities included in the summertime and wintertime flux footprints at YYG were 9 % and



**Figure 4.** Baseline variations of O<sub>2</sub> and CO<sub>2</sub> concentrations at the tower height of 52 m at Yoyogi, Tokyo, Japan, represented by their best-fit curves (black solid lines) to the respective maximum and minimum values during the successive 1-week periods (black dashed lines). Variations of 24 h averaged O<sub>2</sub> and CO<sub>2</sub> concentrations at Minamitorishima, Japan (blue dashed line), and their best-fit curves (blue solid lines), are also shown (updated from Ishidoya et al., 2017).

2 %, respectively (Hirano et al., 2015), and there was no significant solid fuel consumption, such as a coal-fired power-generation plant of which OR is expected to be 1.17 (Keeling, 1988), detected in the footprints. At YYG, the effect of emissions from coal combustion is evaluated simultaneously by the use of aerosol composition monitored every 4 h (Kaneyasu et al., 2020). From these measurements, emission contribution from coal combustion can be detected under a limited meteorological condition, such as a stagnant condition under a weak south-southwesterly wind. This condition occurred only several times a year, mostly from spring to fall. Therefore, the wintertime OR<sub>F</sub> was determined mainly by gas and liquid fuel consumption around the YYG site, given that few vegetation and weak terrestrial biospheric activities took place in the wintertime. If we assume the wintertime OR<sub>F</sub> is determined only by gas and liquid fuel consumption, with OR values of 1.95 and 1.44, respectively, then 45 % of the CO<sub>2</sub> flux during the December to February (DJF) period was driven by gas fuel consumption, with the rest attributed to liquid fuel consumption. It should be noted that the contributions of gas and liquid fuels are expected to be underestimated and overestimated since we have ignored the contribution from human respiration with OR values in the range of 1.0 to 1.4. The respiration quotients (the reciprocal of OR) for carbohydrates, lipid and protein are known to be about

1.0, 0.7 and 0.8, respectively. We also conducted detail analyses to separate out the contributions from the consumption of gas and liquid fuels and human respiration by using the observed CO<sub>2</sub> flux and OR<sub>F</sub> and comparing the results with the CO<sub>2</sub> emission inventory in Sect. 3.3.

Figure 7 also shows that the OR<sub>F</sub> values were systematically larger than OR<sub>atm</sub> throughout the year, except for October 2016 and July 2017. The average OR<sub>F</sub> and OR<sub>atm</sub> during DJF were  $1.67 \pm 0.03$  and  $1.63 \pm 0.02$ , respectively, both of which agree with the OR value of 1.65 calculated using the statistical data of fossil fuel consumption in Tokyo reported by the Agency of Natural Resources and Energy (<http://www.enecho.meti.go.jp/en/>, last access: 18 December 2018), assuming OR values of 1.95, 1.44 and 1.17 for gas, liquid and solid fuel consumption, respectively (hereafter referred to as “OR<sub>ff</sub>”). By using the same procedure as above, the average OR<sub>ff</sub> was calculated to be  $1.52 \pm 0.1$  for the Kanto area of about 17 000 km<sup>2</sup> that includes Tokyo. Therefore, it is suggested that not only OR<sub>F</sub>, but also OR<sub>atm</sub> at YYG, mainly reflected an influence of the fossil fuel consumption in Tokyo rather than that in the wider Kanto area in the wintertime. Both the OR<sub>F</sub> and OR<sub>atm</sub> values in the summer were lower than OR<sub>ff</sub> in Tokyo (1.65), but OR<sub>atm</sub> was also found to be lower than OR<sub>ff</sub> for the Kanto area (1.52). These lower OR<sub>F</sub> and OR<sub>atm</sub> values, compared to those of the

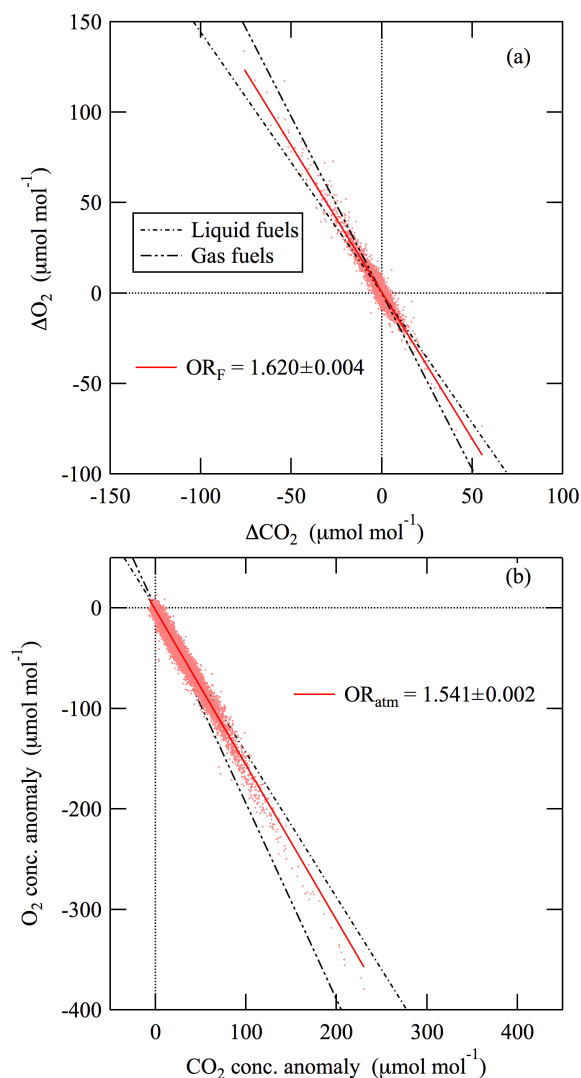


**Figure 5.** (a) Relationship between the  $\Delta\text{O}_2$  and  $\Delta\text{CO}_2$  shown in Fig. 2. The average  $\text{OR}_F$  (see text) for the observation period, derived from the Deming regression fitted to the data, is also shown. (b) Same as in (a) but for the deviations of O<sub>2</sub> and CO<sub>2</sub> concentrations from their baseline variations shown in Fig. 3 and the average  $\text{OR}_{\text{atm}}$  (see text). OR values expected from the consumptions of gas and liquid fuels are also shown.

$\text{OR}_{\text{ff}}$ , suggest that the ratio of fossil fuel combustion to terrestrial biospheric activities and human respiration is lower in the summer than that in the winter. The slightly lower  $\text{OR}_{\text{atm}}$  than  $\text{OR}_F$  at YYG throughout the year is probably due to the higher contribution of the air mass from the Kanto area to  $\text{OR}_{\text{atm}}$  than  $\text{OR}_F$ , since the Kanto area as a whole has lower  $\text{OR}_{\text{ff}}$  than for Tokyo; in addition, the southern Kanto area (including Tokyo) has a larger vegetation coverage of about 50 % than that in the area around the YYG site. From the comparison results of the  $\text{OR}_F$  with  $\text{OR}_{\text{atm}}$  in Figs. 5–7, it is suggested that the  $\text{OR}_{\text{atm}}$  reflects wider footprints of O<sub>2</sub> and CO<sub>2</sub> than  $\text{OR}_F$  for the aggregation periods at least longer

than 12 h to calculate the  $\text{OR}_{\text{atm}}$ . Therefore, to use  $\text{OR}_F$  rather than  $\text{OR}_{\text{atm}}$  is more appropriate to validate inventory-based CO<sub>2</sub> emissions from gas, liquid and solid fuels in the flux footprint.

### 3.3 Consumption of gas and liquid fuels estimated from the observed CO<sub>2</sub> flux and O<sub>2</sub> : CO<sub>2</sub> exchange ratio for net turbulent flux

In this section, we derive average diurnal cycles of  $\text{OR}_F$ , CO<sub>2</sub> and O<sub>2</sub> fluxes and estimate the CO<sub>2</sub> fluxes from gas and liquid fuel consumption separately. Figure 8 shows the average diurnal cycles of  $\Delta\text{O}_2$  and  $\Delta\text{CO}_2$  for each season. To derive the average diurnal cycles, the observed  $\Delta\text{O}_2$  and  $\Delta\text{CO}_2$  values of each day in a season were overlain on top of the values of other days, added up and divided by the number of days in the season. The error bars shown in Fig. 8 indicate  $\pm 1$  standard error ( $\sigma/\sqrt{n}$ ). The  $\Delta\text{O}_2$  and  $\Delta\text{CO}_2$  values vary systematically in opposite phase and take positive and negative values, respectively, indicating transport of O<sub>2</sub> uptake and CO<sub>2</sub> emission signals from the urban area to the overlaying atmosphere throughout the year. Daily maxima of  $\Delta\text{O}_2$  shown in Fig. 8 are higher in the winter than in the summer and occur in the nighttime. These characteristics would be attributable to an enhancement of the anthropogenic O<sub>2</sub> consumption in the winter, while the nighttime decrease in O<sub>2</sub> concentration would be due to the O<sub>2</sub> consumption near the surface and temperature inversion near the surface. It must be noted that the  $\Delta\text{CO}_2$  values in the daytime are nearly zero, while the  $\Delta\text{O}_2$  values are not. The intercepts of the regression lines fitted to the relationship between  $\Delta\text{O}_2$  and  $\Delta\text{CO}_2$  in Fig. 8 are 0.27, 0.41, 0.45 and 0.44  $\mu\text{mol mol}^{-1}$  in DJF, MAM, JJA and SON, respectively. Unfortunately, we did not fix the cause(s) of such biases yet, although it (they) may be related, to some extent, to natural exchange processes between the urban area and the overlaying atmosphere. Therefore, because of these issues, the use of  $\text{OR}_F$ , calculated by applying a Deming regression fitted to 2 h period values of  $\Delta\text{O}_2$  and  $\Delta\text{CO}_2$  of the climatological diurnal cycle (the number of data included in each 2 h periods were 400–800, depending on the season), to determine the relationship between the O<sub>2</sub> and CO<sub>2</sub> fluxes, is preferable. The  $\text{OR}_F$  values plotted in Fig. 8 show diurnal cycles with daytime minima in DJF, MAM and SON, while no clear cycle is found in JJA. From 10:00 to 16:00 local time, the  $\text{OR}_F$  values are in the range of 1.44–1.59 for all seasons. On the other hand, the  $\text{OR}_F$  values from 18:00 to 09:00 local time are more variable, in the range of 1.39–1.74, and are clearly larger in the winter than in the summer.

The observed CO<sub>2</sub> flux and the estimated O<sub>2</sub> flux for each season are shown in Fig. 8. The CO<sub>2</sub> flux shows clear diurnal cycles with two peaks for all seasons, one in the morning and the other in the evening. The shape of the diurnal CO<sub>2</sub> flux cycle, with larger flux in the winter than in the summer, was also found in our previous study at YYG for the period 2012–2013 (Hirano et al., 2015). On the other



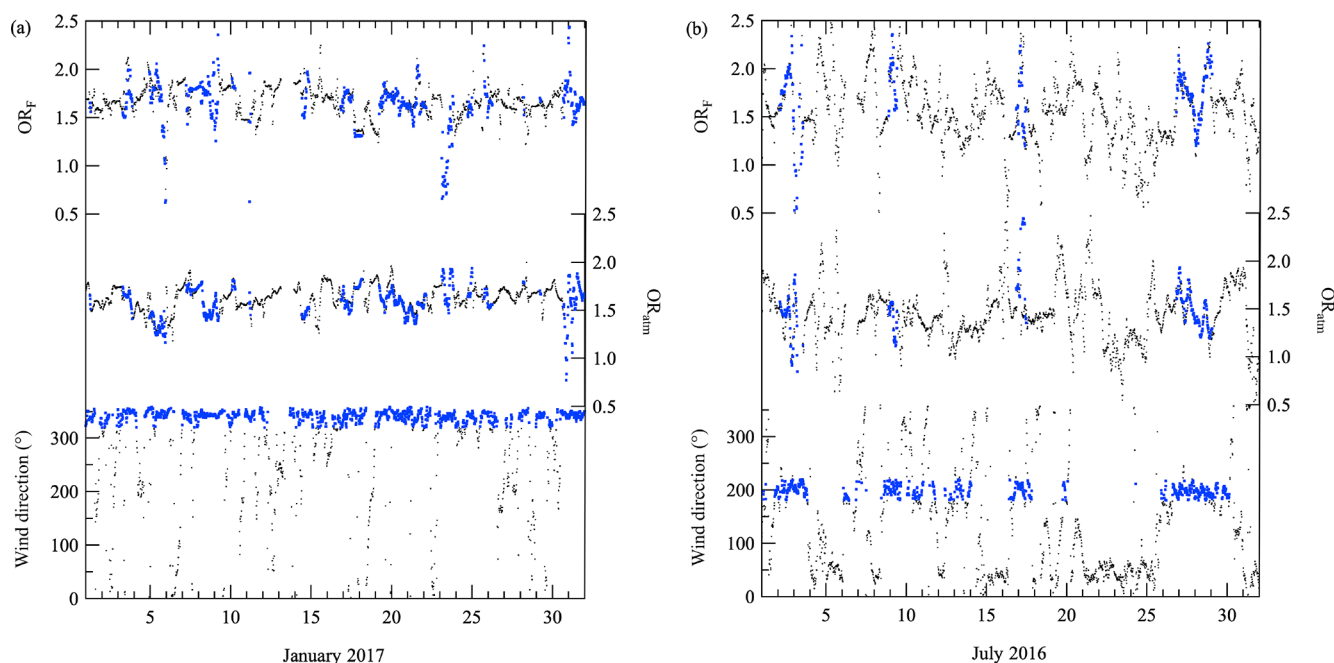


**Figure 6.** (a) OR<sub>F</sub> (black dots, top) calculated by applying Deming regression fitted to  $\Delta\text{O}_2$  and  $\Delta\text{CO}_2$  values during the successive 12 h periods observed in January 2017. The corresponding OR<sub>atm</sub> (black dots, middle) obtained from the deviations of O<sub>2</sub> and CO<sub>2</sub> concentrations from their baseline variations shown in Fig. 4, and the wind directions (black dots, bottom), are also shown. Angles of 90, 180, 270 and 360° for the wind direction denote winds from east, south, west and north, respectively. The OR<sub>F</sub> and OR<sub>atm</sub> obtained from the data observed during the period with the prevailing wind direction (blue dots, bottom) are also shown by blue dots. (b) Same as in (a) but for July 2016.

hand, the O<sub>2</sub> flux shows similar diurnal cycles but in opposite phase with the CO<sub>2</sub> flux. The daily mean CO<sub>2</sub> fluxes were  $15.6 \pm 0.2$ ,  $11.2 \pm 0.1$ ,  $9.3 \pm 0.1$  and  $11.5 \pm 0.1 \mu\text{mol m}^{-2} \text{s}^{-1}$  in DJF, MAM, JJA and SON, respectively, while the respective daily mean O<sub>2</sub> fluxes were  $-25.4 \pm 0.3$ ,  $-17.8 \pm 0.2$ ,  $-14.1 \pm 0.2$  and  $-17.7 \pm 0.2 \mu\text{mol m}^{-2} \text{s}^{-1}$ . The annual average daily mean O<sub>2</sub> flux was  $-16.3 \mu\text{mol m}^{-2} \text{s}^{-1}$ . Steinbach et al. (2011) reported a global dataset of CO<sub>2</sub> emissions and O<sub>2</sub> uptake associated with fossil fuel combustion using the EDGAR inventory with country-level information on OR, based on the fossil fuel consumption data from the UN energy statistics database. The O<sub>2</sub> uptake around Tokyo for the year 2006 has been shown to be about  $e^{16} - e^{17} \text{ kgO}_2 \text{ km}^{-2} \text{ yr}^{-1}$  (Fig. 2 in Steinbach et al., 2011), which corresponds to  $-9$  to  $-24 \mu\text{mol m}^{-2} \text{s}^{-1}$  of O<sub>2</sub> flux and is consistent with those observed in this study. In this regard, the atmospheric O<sub>2</sub> concentration decreased secularly due mainly to fossil fuel combustion at a rate of change of about  $-4 \mu\text{mol yr}^{-1}$  (e.g., Keeling and Manning, 2014), corresponding to  $-0.04 \mu\text{mol m}^{-2} \text{s}^{-1}$  of O<sub>2</sub> flux, assuming  $5.1 \times 10^{14} \text{ m}^2$  for the surface area of the earth,  $5.124 \times 10^{21} \text{ g}$  for the total mass of dry air (Trenberth, 1981) and  $28.97 \text{ g mol}^{-1}$  for the mean molecular weight of dry air. Therefore, the consumption rate of atmospheric O<sub>2</sub> in an urban area of Tokyo is several hundred times larger than the global mean surface consumption rate.

The CO<sub>2</sub> emission inventory was developed based on Hirano et al. (2015) with some modifications. We added human respiration based on the hourly population data (Regional Economy Society Analyzing System, <https://resas.go.jp/>, last access: 11 March 2020). Respiration amount per person was referred from Moriwaki and Kanda (2004). We also added CO<sub>2</sub> emission due to gas consumption by restaurants to the Hirano et al. (2015) inventory, which only accounted for household emission. Monthly gas consumption in restaurants was acquired from the statistical data published by the local government (<http://www.toukei.metro.tokyo.jp/tnenkan/2015/tn15q3i006.htm>, last access: 11 March 2020). Diurnal variation in the gas consumption by the restaurants was obtained from Takahashi et al. (2006) and Takata et al. (2007). We also modified the household gas consumption using the study by Etsuki (2010). As for the traffic, we used traffic load data (<http://www.jartic.or.jp/>, last access: 11 March 2020) which recorded the number of vehicles on the road every hour every day, whereas Hirano et al. (2015) used traffic data for a single day in 2010.

The OR<sub>F</sub> is determined as a ratio of net turbulent fluxes of O<sub>2</sub> and CO<sub>2</sub> from mixed consumption of gas, liquid and solid fuels and terrestrial biospheric activities and human respiration. In this study, the total net turbulent CO<sub>2</sub> flux from the urban area to the overlaying atmosphere is calculated using the eddy correlation method. The CO<sub>2</sub> emission inventories from gas consumption, traffic and human respiration

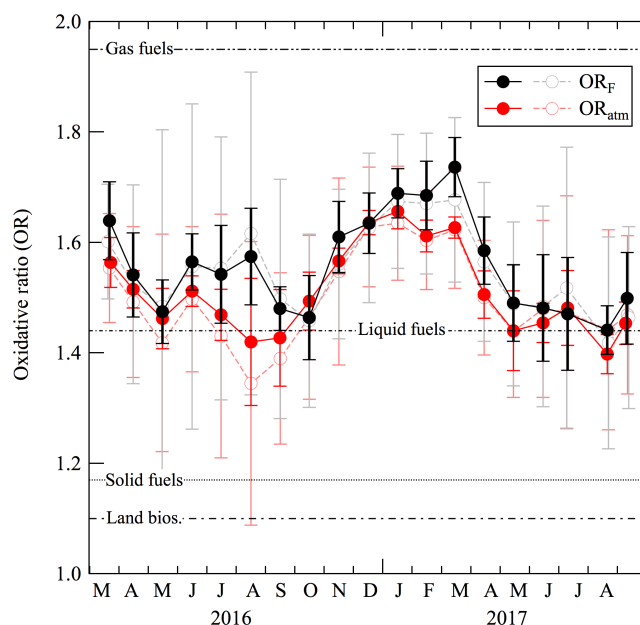


**Figure 7.**  $OR_F$  calculated by applying Deming regression fitted to 1 d (gray open circles) and 1-week (black closed circles) successive  $\Delta O_2$  and  $\Delta CO_2$  values. Also plotted are  $OR_{atm}$  calculated by applying Deming regression fitted to 1 d (light red open circles) and 1-week (dark red closed circles) successive  $O_2$  and  $CO_2$  deviations from their baseline variations shown in Fig. 3. OR values expected from the consumptions of gas, liquid and solid fuels and land biospheric activities are also shown.

have also been updated from the original data published by Hirano et al. (2015). We can then proceed to separate out the  $CO_2$  flux from gas and liquid fuel consumption by using Eq. (4), followed by Eqs. (5)–(6):

$$F_O = -(OR_G \times F_G + OR_L \times F_L + OR_R \times F_R), \quad (5)$$

$$F_C = F_G + F_L + F_R, \quad (6)$$

where  $F_G$ ,  $F_L$  and  $F_R$  ( $\mu\text{mol m}^{-2} \text{s}^{-1}$ ) represent the  $CO_2$  fluxes from gas and liquid fuel consumption and human respiration from the urban area to the overlaying atmosphere, and  $OR_G$ ,  $OR_L$  and  $OR_R$  are the OR values for gas and liquid fuel consumption and human respiration, respectively. We use 1.95, 1.44 and 1.2 for  $OR_G$ ,  $OR_L$  and  $OR_R$ , respectively. For this analysis, it is assumed that the contributions from solid fuel consumption and terrestrial biospheric activities are negligible, given the fact that in the flux footprint area, significant solid fuel consumption is absent and the vegetated area is relatively small. We also assume an  $OR_R$  value of 1.2 as an intermediate value of the reciprocal of respiration quotients for carbohydrates, lipid and protein. We use the  $F_C$  observed by the eddy correlation method and the  $F_R$  obtained from the  $CO_2$  emission inventory to estimate  $F_G$  and  $F_L$ .

Figure 9 shows average diurnal cycles of the observed total  $CO_2$  flux and the  $CO_2$  flux from gas and liquid fuel consumption estimated from Eqs. (4) to (6) for each season. The

average diurnal cycles of the inventory-based total, gas, traffic and human respiration  $CO_2$  fluxes are also shown in the figure. As seen in Fig. 9, similar diurnal cycles with two peaks are found in both the observed and inventory-based total  $CO_2$  fluxes for all seasons. Two peaks of the diurnal cycles are also found in the diurnal cycles of the estimated and inventory-based  $CO_2$  fluxes from gas consumption; however, the evening peaks of the inventory-based flux in MAM, JJA and SON are clearly larger than the estimated values. It is also seen from the figure that the diurnal cycles of inventory-based traffic  $CO_2$  flux do not change significantly throughout the year, while those of the estimated  $CO_2$  flux from liquid fuel consumption show large variabilities, especially in the morning. Such variability may be caused by the smaller  $\Delta O_2$  and  $\Delta CO_2$  values observed during the daytime, compared to those in the nighttime, as well as a rapid change in the atmospheric stability after the daybreak. The actual diurnal cycles of liquid fuel consumption do not seem to change significantly throughout the year, considering the results of the inventory-based traffic  $CO_2$  flux. We therefore consider the standard deviations of the seasonal diurnal cycles of the estimated  $CO_2$  flux from liquid fuel consumption from the annual average diurnal cycle to be the uncertainties for the annual average cycle.

Figure 10 shows the same diurnal cycles of the observed, estimated, and inventory-based  $CO_2$  fluxes as in Fig. 9 but for the annual average cycle. The observed total  $CO_2$  flux is found to be significantly smaller than the inventory-based flux in the evening. Similar discrepancy was also seen in our previous study (Hirano et al., 2015). The main cause of this discrepancy in the evening is likely the much larger inventory-based  $CO_2$  flux from gas consumption than the estimated flux. The estimated  $CO_2$  flux from liquid fuel consumption is somewhat larger than the inventory-based traffic  $CO_2$  flux in the evening, thus contributing to the above-mentioned discrepancy to some extent. Although the uncertainty in the estimated  $CO_2$  flux is large in the morning, the observed peak of the estimated  $CO_2$  flux from gas fuel consumption early in the morning and the gradual increase in the estimated  $CO_2$  flux from liquid fuel consumption over the same time period can be distinguishable. Such temporal variations of the estimated  $CO_2$  flux are reasonable since gas fuel consumption for domestic heating and cooking should increase early in the morning and liquid fuel consumption from the traffic should increase during the morning commute. Consequently, it is confirmed that the simultaneous observations of the  $OR_F$  and  $CO_2$  flux are useful in validating the  $CO_2$  emission inventories developed based on statistical data. However, as shown in Figs. 8–10, a large number of  $\Delta O_2$  and  $\Delta CO_2$  measurement data are needed to derive reliable  $OR_F$  based on an aerodynamic method. If we measure  $O_2$  concentration with high time resolution to determine net turbulent  $O_2$  flux by an eddy correlation method, then it will be possible to derive high-time-resolution  $OR_F$  as a ratio of the observed  $O_2$ -to- $CO_2$  fluxes. Such an innovative technique

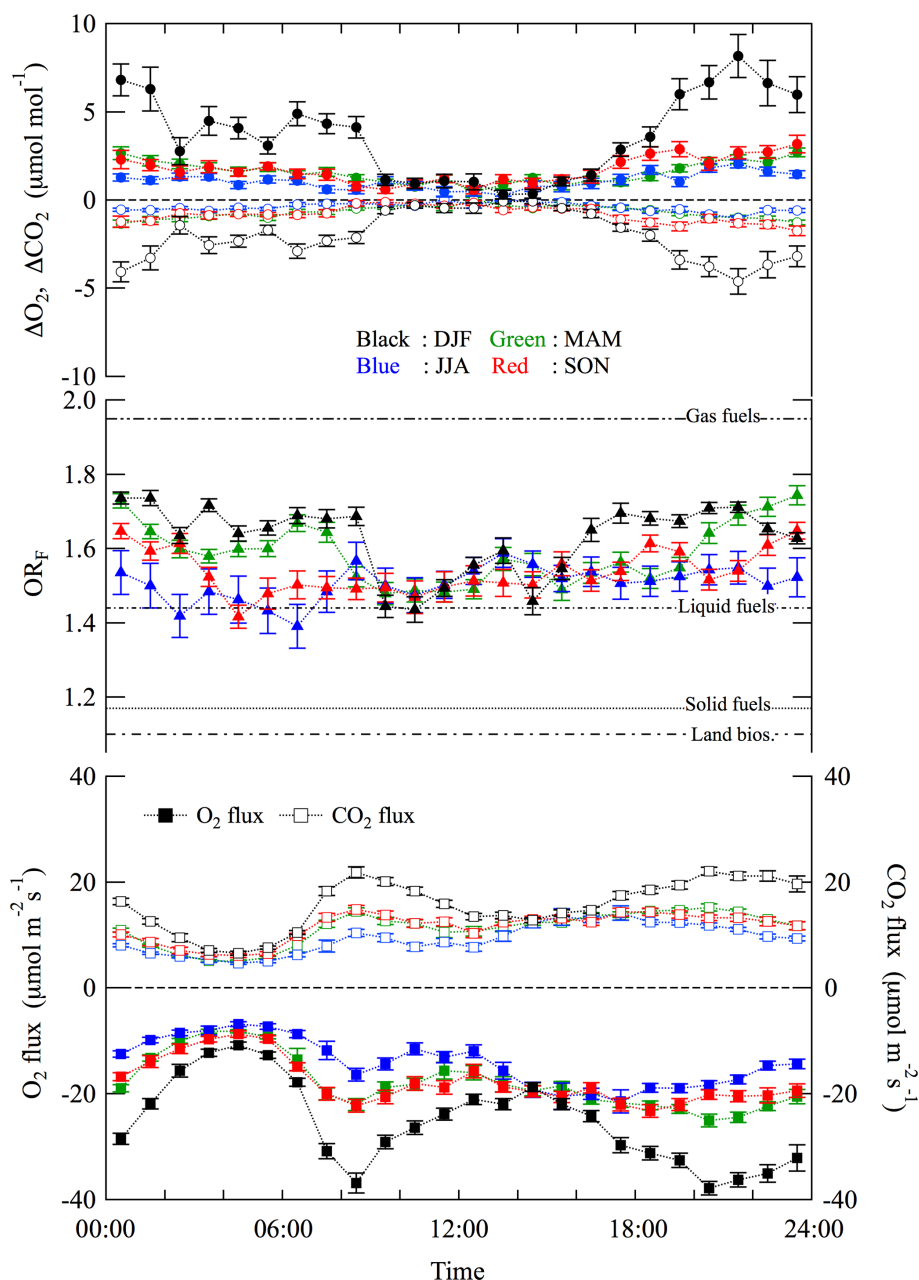


**Figure 8.** Plots of average diurnal cycles of  $\Delta O_2$  (filled circles) and  $\Delta CO_2$  (open circles) for each season: December to February (back), March to May (green), June to August (blue) and September to November (red). Average diurnal cycles of  $OR_F$ , calculated by applying Deming regression fitted to the 2 h period values of  $\Delta O_2$  and  $\Delta CO_2$ , are also plotted seasonally (see text). Average diurnal cycles of the CO<sub>2</sub> flux observed using the eddy correlation method, and those of the O<sub>2</sub> flux calculated from the CO<sub>2</sub> flux and  $OR_F$  values, are also plotted seasonally. Error bars indicate  $\pm 1$  standard error.

will enhance the value of the  $OR_F$  observations significantly for an evaluation of the urban CO<sub>2</sub> emissions.

#### 4 Conclusions

Continuous simultaneous observations of atmospheric O<sub>2</sub> and CO<sub>2</sub> and CO<sub>2</sub> flux have been carried out at the YYG site,

Tokyo, Japan, since March 2016. Sample air was taken from air intakes set at heights of 52 and 37 m of the YYG tower, allowing us to apply an aerodynamic method by using the vertical gradients of the O<sub>2</sub> and CO<sub>2</sub> concentration measurements. We compared  $OR_F$  obtained from the aerodynamic method with  $OR_{\text{atm}}$ , representing OR of the overlaying atmosphere above the urban canopy. We found clear seasonal

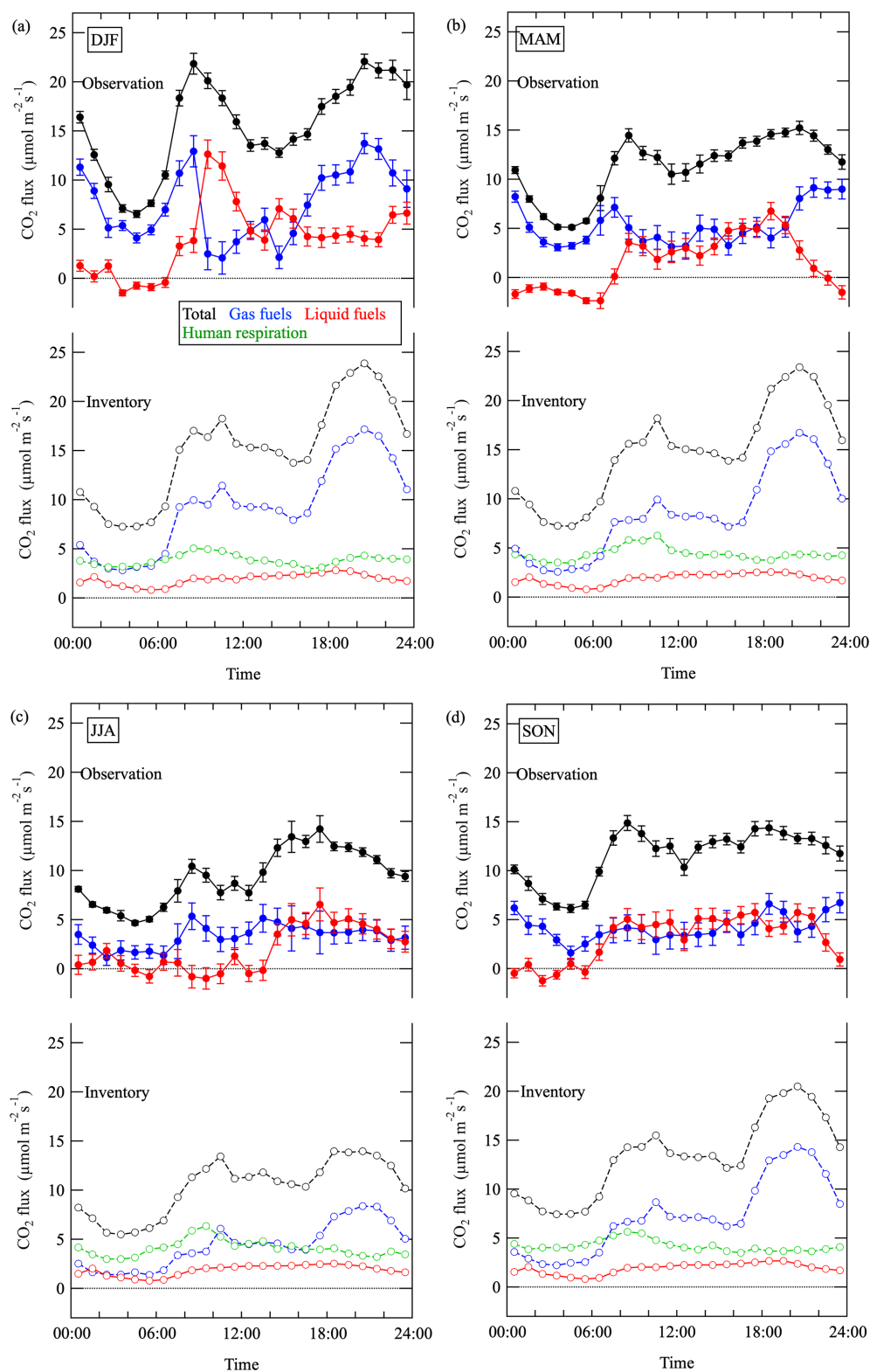


**Figure 9.** Average diurnal cycles of the total CO<sub>2</sub> flux observed using the eddy correlation method (black filled circles) and the estimated CO<sub>2</sub> flux from gas (blue filled circles) and liquid (red filled circles) fuel consumption by using the total CO<sub>2</sub> flux and OR<sub>F</sub> for each season: December to February (a), March to May (b), June to August (c) and September to November (d). Average diurnal cycles of the CO<sub>2</sub> emission inventory of gas consumption (blue open circles), traffic (red open circles), human respiration (green open circles) and their total (black open circles) around YYG are also shown for each season. See text in detail.

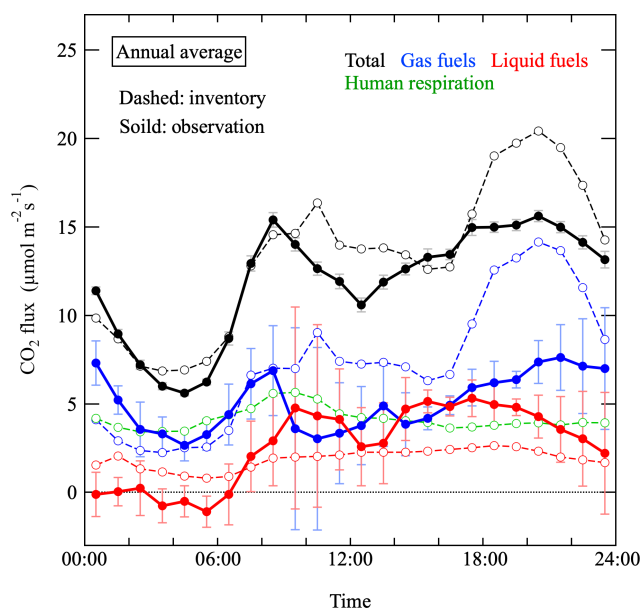


**Figure 10.** Same as in Fig. 9 but for the annual average diurnal cycles. The error bars for the estimated CO<sub>2</sub> flux from liquid fuel consumption are the standard deviations of the diurnal cycles of the flux for respective seasons from the annual average cycle, assuming that the actual diurnal cycles of liquid fuel consumption do not change significantly throughout the year (see text).

variations with wintertime maxima for both OR<sub>F</sub> and OR<sub>atm</sub> as well as slightly higher OR<sub>F</sub> than OR<sub>atm</sub> throughout the year. The annual mean OR<sub>F</sub> and OR<sub>atm</sub> were observed to be 1.62 and 1.54, respectively, falling within the range of the respective average OR values of 1.44 and 1.95 of liquid and gas fuels. The slightly lower OR<sub>atm</sub> than OR<sub>F</sub> throughout the year was probably due to an influence of the air mass from the wider Kanto area to OR<sub>atm</sub> at YYG since the OR value of 1.1 for the terrestrial biospheric activities is lower than those for liquid and gas fuel consumption; in addition, the influence of the vegetation included in the flux footprints at YYG was much smaller than that in the surrounding Kanto area. Therefore, we prefer to use OR<sub>F</sub> rather than OR<sub>atm</sub> to validate the inventory-based CO<sub>2</sub> emissions from gas, liquid and solid fuels in the YYG flux footprint region.

Seasonal variations were seen in the average diurnal OR<sub>F</sub> cycles, showing daytime minima in DJF, MAM and SON, while no clear diurnal cycle was distinguishable in JJA. The daily mean O<sub>2</sub> flux at YYG, calculated from the OR<sub>F</sub> and CO<sub>2</sub> flux, was about  $-25$  and  $-14 \mu\text{mol m}^{-2} \text{s}^{-1}$  in the winter and the summer, respectively, which means the consumption rate of atmospheric O<sub>2</sub> in an urban area of Tokyo is several hundred times larger than the global mean surface consumption rate. We estimated the average diurnal cycles of CO<sub>2</sub> flux from the consumption of gas and liquid fuels for each season, based on the average diurnal cycles of OR<sub>F</sub> and CO<sub>2</sub> flux and the CO<sub>2</sub> emission inventory of human respiration around the YYG site. Discrepancy between the esti-

ated and inventory-based CO<sub>2</sub> fluxes from gas fuel consumption was found to be the main cause of the significantly smaller evening peak of the observed total CO<sub>2</sub> flux than that of the inventory-based total flux. Along with the peak in the estimated CO<sub>2</sub> flux from the gas fuel consumption, the gradual increase in the estimated CO<sub>2</sub> flux from the liquid fuel consumption found in the morning is consistent with the fact that the gas fuel consumption for domestic heating and cooking, and liquid fuel consumption from traffic during commuting, occur in the morning. Therefore, we can use simultaneous observations of OR<sub>F</sub> and CO<sub>2</sub> flux as a powerful tool to validate CO<sub>2</sub> emission inventories obtained from statistical data.

**Data availability.** The data at the YYG site presented in this study can be accessed by contacting the corresponding author.

**Author contributions.** SI designed the study and drafted the manuscript. Measurements of O<sub>2</sub> concentrations, CO<sub>2</sub> concentrations, and CO<sub>2</sub> flux were conducted by SI, SI and YT, and HS, respectively. HS prepared CO<sub>2</sub> emission inventory data. NA prepared standard gas for the O<sub>2</sub> measurements. SI and KT conducted O<sub>2</sub> observations at MNM. HS, NK and HK examined the results and provided feedback on the manuscript. All the authors approved the final manuscript.

**Competing interests.** The authors declare that they have no conflict of interest.

**Acknowledgements.** We thank Takashi Nakajima at Tokai University, Shohei Murayama at the National Institute of Advanced Industrial Science and Technology (AIST), and JANS Co. Ltd. for supporting the observation.

**Financial support.** This study was partly supported by the JSPS KAKENHI (grant nos. 24241008, 15H02814 and 18K01129), the Environment Research and Technology Development Fund (grant no. 1-1909), and the Global Environment Research Coordination System from the Ministry of the Environment, Japan.

**Review statement.** This paper was edited by Thomas Karl and reviewed by three anonymous referees.

## References

- Aoki, N., Ishidoya, S., Matsumoto, N., Watanabe, T., Shimosaka, T., and Murayama, S.: Preparation of primary standard mixtures for atmospheric oxygen measurements with less than  $1 \mu\text{mol mol}^{-1}$  uncertainty for oxygen molar fractions, *Atmos. Meas. Tech.*, 12, 2631–2646, <https://doi.org/10.5194/amt-12-2631-2019>, 2019.



- Aubinet, M., Vesala, T., and Papale, D. (Eds.): Eddy Covariance: A Practical Guide to Measurement and Data Analysis, Springer, the Netherlands, 2012.
- Blaine, T. W., Keeling, R. F., and Paplawsky, W. J.: An improved inlet for precisely measuring the atmospheric Ar/N<sub>2</sub> ratio, *Atmos. Chem. Phys.*, 6, 1181–1184, <https://doi.org/10.5194/acp-6-1181-2006>, 2006.
- Etsuki, R.: SCADA system of Tokyo Gas for wide-area city gas distribution, in: Proceedings of the 53rd Japan Joint Automatic Control Conference, Kochi, Japan, November 2010, 46, 1099–1102, 2010.
- Goto, D., Morimoto, S., Ishidoya, S., Ogi, A., Aoki, S., and Nakazawa, T.: Development of a high precision continuous measurement system for the atmospheric O<sub>2</sub>/N<sub>2</sub> ratio and its application at Aobayama, Sendai, Japan, *J. Meteorol. Soc. Jpn.*, 91, 179–192, 2013a.
- Goto, D., Morimoto, S., Aoki, S., and Nakazawa, T.: High precision continuous measurement system for the atmospheric O<sub>2</sub>/N<sub>2</sub> ratio at Ny-Ålesund, Svalbard and preliminary observational results, *Nankyo Shiryō (Antarct. Rec.)*, 57, 17–27, 2013b.
- Goto, D., Morimoto, S., Aoki, S., Patra, P. K., and Nakazawa, T.: Seasonal and short-term variations in atmospheric potential oxygen at Ny-Ålesund, Svalbard, *Tellus B*, 69, 1311767, <https://doi.org/10.1080/16000889.2017.1311767>, 2017.
- Hirano, T., Sugawara, H., Murayama, S., and Kondo, H.: Diurnal variation of CO<sub>2</sub> flux in an urban area of Tokyo, *SOLA*, 11, 100–103, 2015.
- Hoshina, Y., Tohjima, Y., Katsumata, K., Machida, T., and Nakaoka, S.: In situ observation of atmospheric oxygen and carbon dioxide in the North Pacific using a cargo ship, *Atmos. Chem. Phys.*, 18, 9283–9295, <https://doi.org/10.5194/acp-18-9283-2018>, 2018.
- Ishidoya, S. and Murayama, S.: Development of high precision continuous measuring system of the atmospheric O<sub>2</sub>/N<sub>2</sub> and Ar/N<sub>2</sub> ratios and its application to the observation in Tsukuba, Japan, *Tellus B*, 66, 22574, <https://doi.org/10.3402/tellusb.v66.22574>, 2014.
- Ishidoya, S., Sugawara, S., Morimoto, S., Aoki, S., Nakazawa, T., Honda, H., and Murayama, S.: Gravitational separation in the stratosphere – a new indicator of atmospheric circulation, *Atmos. Chem. Phys.*, 13, 8787–8796, <https://doi.org/10.5194/acp-13-8787-2013>, 2013a.
- Ishidoya, S., Murayama, S., Takamura, C., Kondo, H., Saigusa, N., Goto, D., Morimoto, S., Aoki, N., Aoki, S., and Nakazawa, T.: O<sub>2</sub> : CO<sub>2</sub> exchange ratios observed in a cool temperate deciduous forest ecosystem of central Japan, *Tellus B*, 65, 21120, <https://doi.org/10.3402/tellusb.v65i0.21120>, 2013b.
- Ishidoya, S., Murayama, S., Kondo, H., Saigusa, N., Kishimoto-Mo, A. W., and Yamamoto, S.: Observation of O<sub>2</sub> : CO<sub>2</sub> exchange ratio for net turbulent fluxes and its application to forest carbon cycles, *Ecol. Res.*, 30, 225–234, 2015.
- Ishidoya, S., Tsuboi, K., Murayama, S., Matsueda, H., Aoki, N., Shimosaka, T., Kondo, H., and Saito, K.: Development of a continuous measurement system for atmospheric O<sub>2</sub>/N<sub>2</sub> ratio using a paramagnetic analyzer and its application in Minamitorishima Island, Japan, *SOLA*, 13, 230–234, 2017.
- Kaneyasu, N., Ishidoya, S., Terao, Y., Mizuno, Y., and Sugawara, H.: Estimation of PM<sub>2.5</sub> Emission Sources in the Tokyo Metropolitan Area by Simultaneous Measurements of Particle Elements and Oxidative Ratio in Air, *ACS Earth Space Chem.*, 4, 297–304, 2020.
- Keeling, R. F. and Manning, A. C.: Studies of recent changes in atmospheric O<sub>2</sub> content, in *Treatise on Geochemistry*, Vol. 5, 2nd Edn., Elsevier, Amsterdam, 385–404, 2014.
- Keeling, C. D., Piper, S. C., Whorf, T. P., and Keeling, R. F.: Evolution of natural and anthropogenic fluxes of atmospheric CO<sub>2</sub> from 1957 to 2003, *Tellus B*, 63, 1–22, 2011.
- Keeling, R. F.: Development of an Interferometric Oxygen Analyzer for Precise Measurement of the Atmospheric O<sub>2</sub> Mole Fraction, PhD thesis, Harvard University, Cambridge, 1988.
- Keeling, R. F. and Shertz, S. R.: Seasonal and interannual variations in atmospheric oxygen and implications for the global carbon cycle, *Nature*, 358, 723–727, 1992.
- Keeling, R. F., Bender, M. L., and Tans, P. P.: What atmospheric oxygen measurements can tell us about the global carbon cycle, *Global Biogeochem. Cy.*, 7, 37–67, 1993.
- Linnet, K.: Estimation of the linear relationship between the measurements of two methods with proportional errors, *Stat. Med.*, 9, 1463–1473, 1990.
- Linnet, K.: Performance of Deming regression analysis in case of misspecified analytical error ratio in method comparison studies, *Clin. Chem.*, 44, 1024–1031, 1998.
- Machida, T., Tohjima, Y., Katsumata, K., and Mukai, H.: A new CO<sub>2</sub> calibration scale based on gravimetric one-step dilution cylinders in National Institute for Environmental Studies-NIES 09 CO<sub>2</sub> scale, Paper presented at: Report of the 15th WMO Meeting of Experts on Carbon Dioxide Concentration and Related Tracer Measurement Techniques, September 2009, Jena, Germany, WMO/GAW Rep. 194, edited by: Brand, W., 165–169, WMO, Geneva, Switzerland, 2011.
- Mauder, M. and Foken, T.: Impact of post-field data processing on eddy covariance flux estimates and energy balance closure, *Meteorol. Z.*, 15, 597–609, 2006.
- Mitchell, L. E., Lin, J. C., Bowling, D. R., Pataki, D. E., Strong, C., Schauer, A. J., Bares, R., Bush, S. E., Stephens, B. B., Mendoza, D., Mallia, D., Holland, L., Gurney, K. R., and Ehleringer, J. R.: Long-term urban carbon dioxide observations reveal spatial and temporal dynamics related to urban characteristics and growth, *P. Natl. Acad. Sci. USA*, 115, 2912–2917, <https://doi.org/10.1073/pnas.1702393115>, 2018.
- Moriwaki, R. and Kanda, M.: Seasonal and Diurnal Fluxes of Radiation, Heat, Water Vapor, and Carbon Dioxide over a Suburban Area, *J. Appl. Meteorol.*, 43, 1700–1710, 2004.
- Nakazawa, T., Aoki, S., Murayama, S., Fukabori, M., Yamanouchi, T., and Murayama, H.: The concentration of atmospheric carbon dioxide at Japanese Antarctic station, Syowa, *Tellus B*, 43, 126–135, 1991.
- Neftel, A., Spirig, C., and Ammann, C.: Application and test of a simple tool for operational footprint evaluations, *Environ. Pollut.*, 152, 644–652, 2008.
- Sargent, M., Barrera, Y., Nehrorn, T., Hutyra, L. R., Gately, C. K., Jones, T., McKain, K., Sweeney, C., Hegarty, J., Hardiman, B., Wang, J. A., and Wofsy, S. C.: Anthropogenic and biogenic CO<sub>2</sub> fluxes in the Boston urban region, *P. Natl. Acad. Sci. USA*, 115, 7491–7496, <https://doi.org/10.1073/pnas.1803715115>, 2018.
- Schmid, H. P.: Source areas for scalars and scalar fluxes, *Bound.-Lay. Meteorol.*, 67, 293–318, 1994.

- Severinghaus, J.: Studies of the terrestrial O<sub>2</sub> and carbon cycles in sand dune gases and in biosphere 2, PhD thesis, Columbia University, New York, 1995.
- Song, T. and Wang, Y.: Carbon dioxide fluxes from an urban area in Beijing, *Atmos. Res.*, 106, 139–149, 2012.
- Steinbach, J., Gerbig, C., Rödenbeck, C., Karstens, U., Minejima, C., and Mukai, H.: The CO<sub>2</sub> release and Oxygen uptake from Fossil Fuel Emission Estimate (COFFEE) dataset: effects from varying oxidative ratios, *Atmos. Chem. Phys.*, 11, 6855–6870, <https://doi.org/10.5194/acp-11-6855-2011>, 2011.
- Takahashi, M., Imamura, E., Urabe, W., and Miyanaga, T.: A Measurement Survey of Electricity, Gas and Hot Water Demand at a Restaurant and Analysis of Time Variation in the End-use Energy Demand, Socio-economic Research Center, Rep. No. Y05024, Central Research Institute of Electric Power Industry, Tokyo, 2006.
- Takata, H., Murakawa, S., and Takana, A.: Analysis on the loads of hot water supply demands in restaurants, *J. Environ. Eng. (Transactions of AIJ)*, 616, 59–65, 2007.
- Tohjima, Y., Machida, T., Watai, T., Akama, I., Amari, T., and Moriwaki, Y.: Preparation of gravimetric standards for measurements of atmospheric oxygen and re-evaluation of atmospheric oxygen concentration, *J. Geophys. Res.*, 110, D11302, <https://doi.org/10.1029/2004JD005595>, 2005a.
- Tohjima, Y., Mukai, H., Machida, T., Nojiri, Y., and Gloor, M.: First measurements of the latitudinal atmospheric O<sub>2</sub> and CO<sub>2</sub> distributions across the western Pacific, *Geophys. Res. Lett.*, 32, L17805, <https://doi.org/10.1029/2005GL023311>, 2005b.
- Trenberth, K. E.: Seasonal variations in global sea level pressure and the total mass of the atmosphere, *J. Geophys. Res.*, 86, 5238–5246, 1981.
- Velasco, E., Pressley, S., Grivicke, R., Allwine, E., Coons, T., Foster, W., Jobson, B. T., Westberg, H., Ramos, R., Hernández, F., Molina, L. T., and Lamb, B.: Eddy covariance flux measurements of pollutant gases in urban Mexico City, *Atmos. Chem. Phys.*, 9, 7325–7342, <https://doi.org/10.5194/acp-9-7325-2009>, 2009.
- van der Laan, S., van der Laan-Luijkx, I. T., Zimmermann, L., Conen, F., and Leuenberger, M.: Net CO<sub>2</sub> surface emissions at Bern, Switzerland inferred from ambient observations of CO<sub>2</sub>,  $\delta(\text{O}_2/\text{N}_2)$ , and <sup>222</sup>Rn using a customized radon tracer inversion, *J. Geophys. Res.-Atmos.*, 119, 1580–1591, <https://doi.org/10.1002/2013JD020307>, 2014.
- Ward, H. C., Evans, J. G., and Grimmond, C. S. B.: Multi-season eddy covariance observations of energy, water and carbon fluxes over a suburban area in Swindon, UK, *Atmos. Chem. Phys.*, 13, 4645–4666, <https://doi.org/10.5194/acp-13-4645-2013>, 2013.
- Webb, E. K., Pearman, G. I., and Leuning, R.: Correction of flux measurements for density effects due to heat and water vapor transfer, *Q. J. Roy. Meteor. Soc.*, 106, 85–100, 1980.
- Wilczak, J. M., Oncley, S. P., and Stage, S. A.: Sonic anemometer tilt correction algorithms, *Bound.-Lay. Meteorol.*, 99, 127–150, 2001.
- Yamamoto, S., Murayama, S., Saigusa, N., and Kondo, H.: Seasonal and inter-annual variation of CO<sub>2</sub> flux between a temperate forest and the atmosphere in Japan, *Tellus B*, 51, 402–413, 1999.